# ERRATUM

The June 1994 issue of *Pure and Applied Chemistry* (Volume 66, No. 6) included the articles 'Theoretical basis of non-equilibrium near atmospheric pressure plasma chemistry' by A. A. Fridman and V. D. Rosanov, and 'Modelling of dielectric barrier discharge chemistry' by B. Eliasson, W. Egli and U. Kogelschatz. Unfortunately, the front pages of these two papers were transposed during production so that the body of both papers was printed out of position within the issue, and given the wrong page numbers and running headlines.

Both articles are reproduced in their entirety on the following pages with the correct page numbers and running headlines. A correct version of the contents page is also reproduced. These pages should be used to replace those in the faulty printed copies.

Blackwell Scientific Publications apologizes to the authors for this error, and to readers who will have experienced some confusion.

*Pure & Appl. Chem.*, Vol. 66, No.6, pp. 1275-1286, 1994.
Printed in Great Britain.


# Modelling of dielectric barrier discharge chemistry

B. Eliasson, W. Egli and U. Kogelschatz

ABB Corporate Research, CH-5405 Baden, Switzerland

Abstract

The discharge physics and plasma chemistry of dielectric barrier discharges (silent discharges) is discussed. Numerical models describing electrical breakdown, microdischarge formation and the ensuing free radical chemistry are presented. Applications ranging from ozone generation, excimer UV lamps and $CO_2$ lasers to surface treatment and pollution control are described. Experimental and modelling results on $CO_2$ hydrogenation in dielectric barrier discharges are also presented.

## INTRODUCTION

Dielectric barrier discharges or barrier discharges, frequently also referred to as silent discharges, have been utilized for more than a century. Early investigations originally started by Siemens (1) in 1857 concentrated on the generation of ozone by subjecting a stream of oxygen or air to the influence of a dielectric barrier discharge (DBD). Ozone and nitrogen oxide formation in DBDs became an important research issue for many decades (2-4). The names of Warburg (5,6) and Becker (7,8) in Germany, Otto (9) in France, of Briner et al. (10) in Switzerland, of Philippov and his group in Russia (11), of Devins (12) in the United States, Lunt (13) in England and Fuji et al. (14) in Japan, should be mentioned in this connection. More recent references can be found in a book by Samoilovich et al.(15) and in some review papers by Eliasson and Kogelschatz (16-19). As of today, ozone generation is still the major industrial application of DBDs with thousands of installed ozone generating facilities based on this principle. For this reason the dielectric barrier discharge is sometimes also referred to as the ozonizer discharge.

In recent years novel applications of DBDs with respect to pumping of $CO_2$ lasers (20-22) and excimer lamps (23-28), flue gas treatment (29-31), surface modification (32-34), pollution control (17, 35-38), $H_2S$ decomposition (39) and $CO_2$ hydrogenation (40, 41) have been proposed. All these applications take advantage of a mature technology originally developed for ozone generators. Its main advantage is that large gas flows at about atmospheric pressure can be subjected to nonequilibrium plasma conditions with only negligible increase of the enthalpy of the feed gas. With all these diverse applications in mind the dielectric barrier discharge configuration will be discussed in a very general sense as a plasmachemical reactor. Special discharge properties will be described as well as charged particle reactions and the free radical chemistry initiated by the gas discharge. Several results are presented concerning the modelling of dielectric barrier discharge chemistry in different gases.

## THE DIELECTRIC BARRIER DISCHARGE

In this section the electrode configurations and typical operating conditions of DBDs are described. When the electrical field in the discharge gap is high enough to cause electrical breakdown a large number of microdischarges are observed if the pressure is of the order of 1 bar. This is a typical pressure range for ozone generation, excimer formation as well as for flue gas treatment. Plasma formation and electrical conductivity is restricted to these microdischarges while the space in between is not ionized and serves only as a background reservoir for the energy dissipated in the microdischarges and for the long-lived species created. Fig. 1 shows a frame from a video taken at very low power density. It shows microdischarges in an annular discharge gap between two quartz cylinders. Visual access was provided by a wire mesh used as

the outer electrode. The gap spacing was 5.5 mm, the operating frequency 200 kHz and the exposure time of the video frame 16 ms.

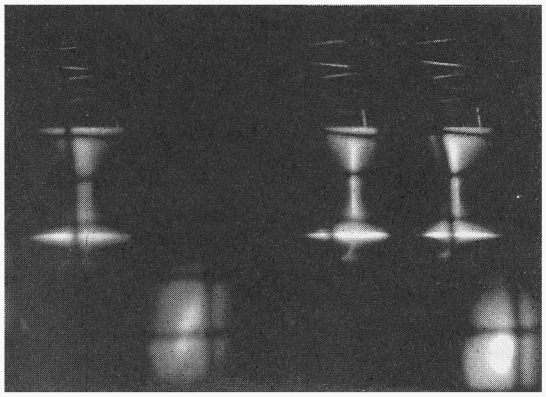

Fig. 1: Video frame showing microdischarges.

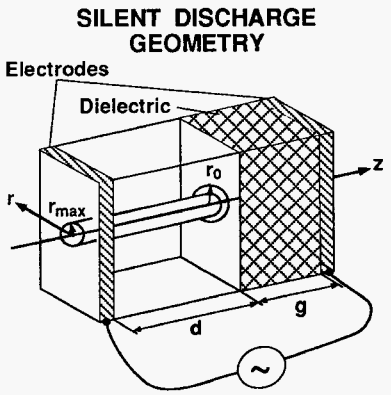


Fig. 2: Diagram of electrode configuration with a microdischarge channel.

Fig. 2 shows schematically a microdischarge in a discharge gap bordered by one dielectric and one metal electrode, a configuration normally encountered in ozone generators. In other applications like $CO_2$ lasers and excimer lamps both electrodes may be covered with dielectrics. The preferred materials for the dielectric barrier are glass or quartz, in special cases also ceramics, enamel or even polymer coatings. Besides the planar configuration sketched in Fig. 2 also annular discharge gaps between cylindrical electrodes and dielectrics are used in many technical applications.

The discharge gap itself has a typical width of a few mm: about 1 mm for ozone generators, a few mm for excimer lamps, and up to 50 mm for $CO_2$ lasers. To initiate a discharge in such a discharge gap filled with a gas at atmospheric pressure, voltages in the range of a few kV are required. Since the current has to pass the dielectric in the form of a displacement current (capacitive coupling), alternating voltages are required to drive a DBD. Although traditionally the line frequency was the obvious choice, modern DBD equipment often runs at higher frequencies. Ozone generators use thyristor-controlled inverters generating square-wave currents in the kHz range, while excimer lamps and $CO_2$ lasers use transistorized switch-mode power supplies with essentially sinusoidal output voltages. Their frequencies can go up to about 1 MHz.

The gas can either flow through the DBD (ozone generation, $CO_2$ conversion, $H_2S$ disposal, pollution control) or it can be recirculated ($CO_2$ lasers) or even fully encapsulated (excimer lamps). In most high-power applications efficient cooling of at least one of the electrodes is used.

## BREAKDOWN PHENOMENA AND DISCHARGE PHYSICS

At atmospheric pressure electrical breakdown in a large number of statistically distributed microdischarges is the normal situation for most gases in DBD configurations. It should be mentioned, however, that discharge plasmas which are apparently homogeneous can be obtained in the same electrode configurations if the pressure is lowered. These discharges are normally referred to as RF discharges and have found widespread applications in the semiconductor industry for plasma etching and plasma deposition procedures. Even at elevated pressures close to 1 bar fairly homogeneous discharges can be obtained if the discharge is pulsed, if large amounts of diluents like He or Ne are added (32, 34, 42, 43) or if special additives are used (44).

The normal appearance of dielectric barrier discharges at elevated pressure, however, is that shown in Fig. 1. It is characterized by a large number of short-lived microdischarges. Each microdischarge has an almost cylindrical plasma channel of typically 100 μm radius and spreads into a larger surface discharge at the dielectric surface. By applying an electric field larger than the breakdown field local breakdown in the gap is initiated. At the given conditions propagating electron avalanches quickly produce such a high space charge that self-propagating streamers are generated (16). This condition is typically met before the initial

electron avalanche reaches the opposite electrode. The field enhancement at the streamer head, moving much faster than the electron drift velocity, is reflected at the anode and travels back to the cathode where, within a fraction of 1 ns, an extremely thin cathode layer is formed. At this time a conductive channel, which can be charaterized as a transient glow discharge, bridges the gap. At atmospheric pressure electron densities of $10^{14}$ to $10^{15}$ $cm^{-3}$ are reached. The thickness of the cathode layer reaches only a few μm (45, 46). Charge accumulation at the dielectric surface results in a local reduction of the electric field which chokes the current flow in a microdischarge typically within less than 100 ns. For a given gas, the choking effect depends on the extension of the surface discharge and the properties of the dielectric barrier. If the external voltage is still rising, additional microdischarges will preferentially strike at other locations with higher electric fields. Thus, the dielectric serves a dual purpose. It limits the amount of charge and energy imparted to an individual microdischarge and, at the same time, distributes the microdischarges over the entire electrode area. Typical charges transported by individual microdischarges are of the order of nC, typical energies of the order of μJ.

It is important to realize that some control of the plasma characteristics is possible by making use of special gas properties, adjusting the pressure or changing the electrode geometry or the properties of the dielectrics. The radius $r_{max}$ of the microdischarge column, for example, depends on the gas density n and on the gas properties. $r_{max}$ is proportional to the reciprocal value of the product of the gas density n and the derivative of the effective ionization coefficient $\bar{\alpha}$ with respect to the reduced electric field E/n (at breakdown) (47). Fig. 3 shows $\bar{\alpha}/n$ for different gases. The effective ionization coefficient $\bar{\alpha}$ is obtained from the ionization coefficient $\alpha$ and the attachment coefficient $\eta$. Its value corresponds to $(\alpha - \eta)$. The sharp decay of the curves of $O_2$ and $CO_2$ below breakdown in Fig. 3 is due to electron attachment in these electronegative gases. From these curves it is evident that the radii of the microdischarge channels can be grouped in the following order:

oxygen < carbon dioxide < air < nitrogen < xenon < helium.

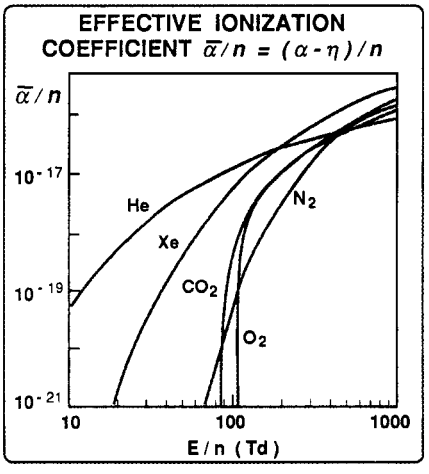


Fig. 3: Effective ionization coefficient indifferent gases.

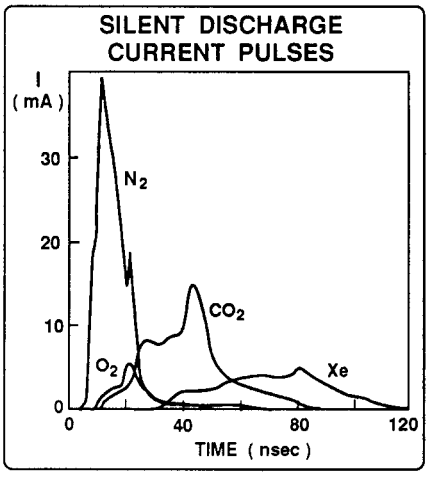


Fig. 4: Microdischarge current pulses in different gases.

The shape of the current pulse of a microdischarge is influenced by the gas properties and by the relative overvoltage applied to the discharge gap. Fig. 4 shows current pulses in different gases, all calculated for 1 bar. The reduced fields were 230 Td, 155 Td, 155 Td and 100 Td for $N_2$, $O_2$, $CO_2$ and Xe respectively. Fig. 5 shows three current pulses in $CO_2$ at different voltages. Surprisingly enough, the transported charge in these three pulses is practically identical.

The total charge Q in a microdischarge depends on the gas properties and can be influenced by the gap spacing and by the properties of the dielectric. Q is proportional to the width of the discharge gap d, and to the quantity $\varepsilon/g$ ($\varepsilon$: relative permittivity, g: thickness of dielectric). Recently, the latter relation was experimentally checked to hold up to extreme $\varepsilon$-values of about 1000 (48). Contrary to what one might expect, Q **does not** depend on the gas density n (16).

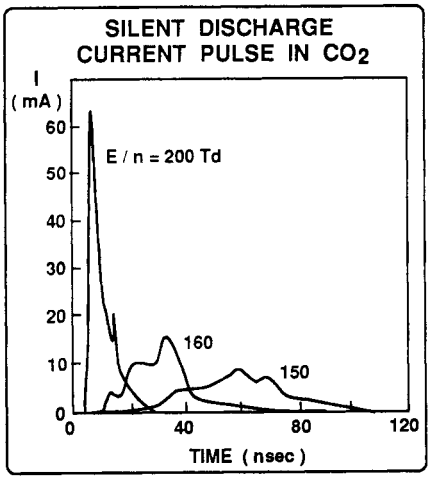


Fig. 5: Microdischarge current pulses in $CO_2$ at different overvoltages.

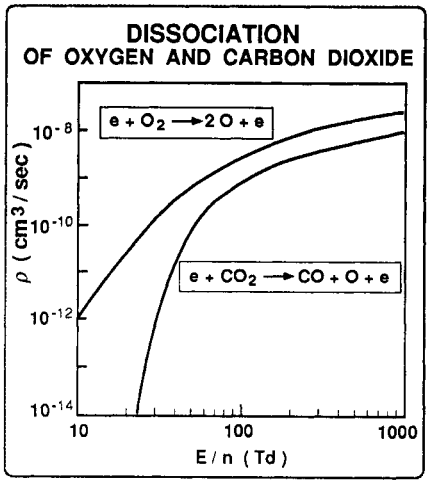


Fig. 6: Dissociation rate coefficient in $O_2$ and $CO_2$.

## MICRODISCHARGE CHEMISTRY

The initial phases of microdischarge formation are characterized by electron multiplication, space charge formation and ionization, dissociation and excitation processes initiated by energetic electrons. The ionic and excited atomic and molecular species initiate chemical reactions that finally result in the synthesis of a desired species (e.g. ozone, excimers, methanol) or the destruction of pollutants (e.g. $H_2S$, $NO_x$, $SO_x$, VOCs etc.). The resulting chemistry can be dominated by charged particle reactions in which case the term plasma chemistry would adequately describe the situation. This situation occurs in many low pressure discharges. In the majority of DBD applications, however, most charged particles decay before any major chemical changes happen. In this case it is more appropriate to speak of a free radical chemistry involving neutral species like atoms, molecular fragments and excited molecules. In any case, discharge activity and energy dissipation occurs only within the microdischarges and sets the initial conditions for the ensuing chemical reactions. Thus, a correct description of the physical processes during breakdown and microdischarge formation is prerequisite for a detailed understanding of DBD chemistry.

In many cases the first step is a dissociation of the initial species by electron collisions. Fig. 6 shows the rate coefficients for this dissociation process for the two important gases $O_2$ and $CO_2$ as a function of the reduced electric field. The dissociation of $O_2$ (49-53) has been investigated in connection with ozone

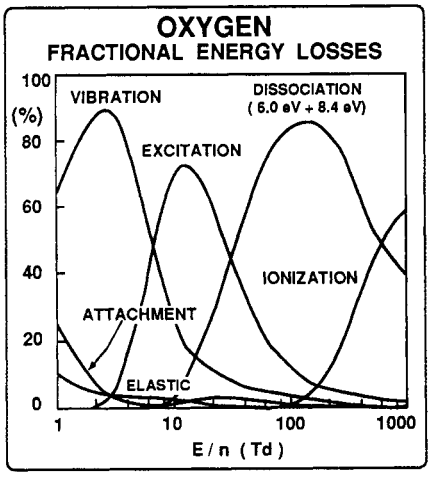


Fig. 7: Fractional energy losses in $O_2$.

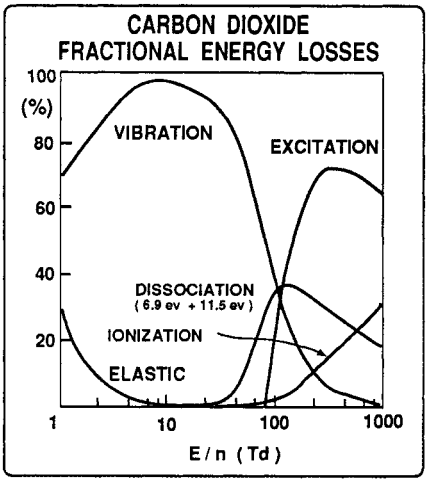


Fig. 8: Fractional energy losses in $CO_2$.

generation and the properties of $CO_2$ (54-58) have been studied with the aim of optimizing $CO_2$ lasers. One important question is the efficiency of the dissociation process with respect to energy consumption. It can be answered by computing fractional energy losses for the different processes involved. Fig. 7 demonstrates that the dissociation of oxygen by electron impact can be highly efficient (up to 85%) provided that the reduced electric field is in the range of 100 - 300 Td (1 Townsend or Td corresponds to $10^{-17}$ Vcm$^2$). This range corresponds to average electron energies of about 4 to 8 eV. In $CO_2$ (Fig. 8), on the other hand, at most 40% of the electron energy can be utilized for the dissociation process under favourable conditions. The efficiency of the different processes involved depends on their cross sections for electron collisions and on the electron energy distribution function.

## NUMERICAL MODELLING

The problem of calculating the transition of an insulating gas to a conductive plasma, i.e. electrical breakdown, has been treated by several authors (16, 45, 46, 59-64). After compiling the dominant electron collision cross sections of the gas under investigation in a first step the Boltzmann equation is solved to obtain the electron energy distribution function. Then the relevant rate coefficients for the electronic reactions like excitation, dissociation, ionization, and attachment are calculated and tabulated as a function of the reduced field E/n.

By applying an electric field larger than the breakdown field and releasing a small number of initial electrons at a certain location of the cathode the evolution of a microdischarge can be calculated. We use a two-dimensional time dependent model solving the continuity equation for the charged particles and computing the local electric field with a fast Poisson solver in cylindrical coordinates. The boundary conditions at the dielectric are given by the charge deposited at the dielectric surface. By performing these calculations as a function of time and space and, at the same time, considering the already tabulated rate coefficients one obtains the distribution of all charged and excited species during the entire microdischarge. After the termination of the microdischarge caused by the decay of charged particles the excited species continue to react to form other radicals and new molecules. Approximate time scales for the different processes involved in a gas at about atmospheric pressure are given in Fig. 9 . Roughly speaking, electrons reach equilibrium conditions corresponding to the applied field within ps, microdischarges occur at a ns time scale, free radical reactions may need ms and ground state chemistry even longer to reach equilibrium conditions. The rate coefficients for electronic collisions depend on the reduced electric field E/n. The use of tabulated values as described above is only justified if equilibrium conditions are reached much faster than the relevant field changes occur. Fig. 10 shows a Monte Carlo simulation of electrons in oxygen at atmospheric pressure (65). Equilibrium is reached in less than 20 ps under these conditions. This is roughly 1000 times faster than the microdischarge pulses calculated in Fig. 4 and Fig. 5.

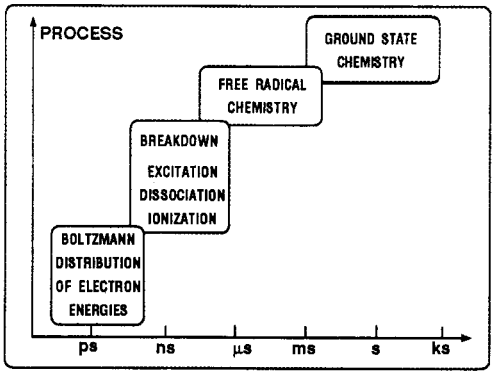


Fig. 9: Schematic representation of processes and time scales involved (p ≈ 1 bar).

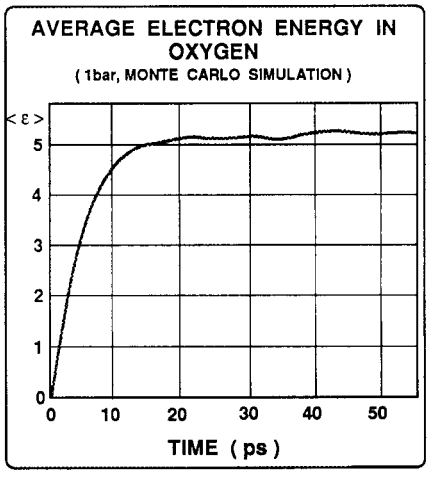


Fig. 10: Monte Carlo simulation of electrons in oxygen (p = 1 bar, T = 300 K, E/n = 100 Td).

Fig. 11 shows results of our two-dimensional model calculations in $CO_2$. The spatial distribution of CO radicals, which according to the dissociation equation (Fig. 6)

$$e + CO_2 \rightarrow e + CO + O \quad (1)$$

is identical to the distribution of oxygen atoms, is plotted for different times during microdischarge formation and after its termination. The current pulse corresponds to the middle pulse of Fig. 5 which peaks at 30 ns and is essentially terminated at 70 ns. The CO distribution is obtained from a time integral of the electron density times the dissociation rate coefficient. It clearly shows the region of the microdischarge channel and the distribution of surface charges at the dielectric surface.

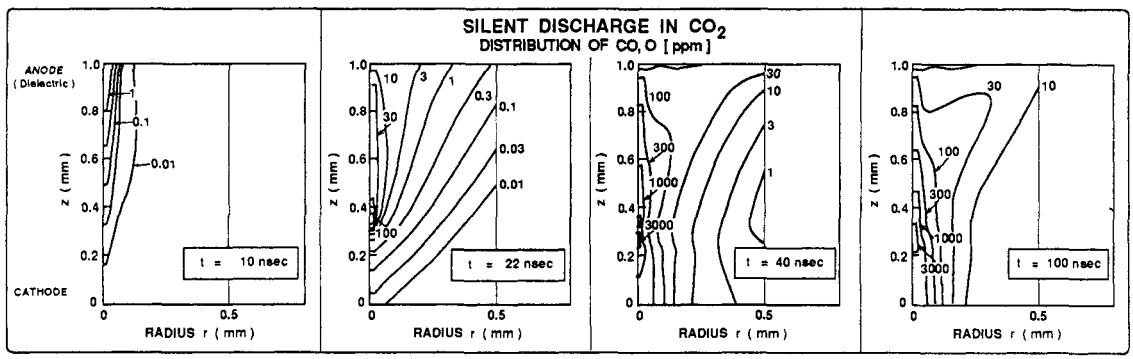


Fig. 11: Concentration of CO at different times during microdischarge evolution.

Fig. 12 shows the total number of CO molecules or O atoms formed in a single microdischarge as a function of time. Fig. 13 shows relative concentrations of these species as a function of the axial coordinate z during the development of a microdischarge. These concentrations were averaged in the radial direction for $0 \leq r \leq R \approx 0.8$ mm.

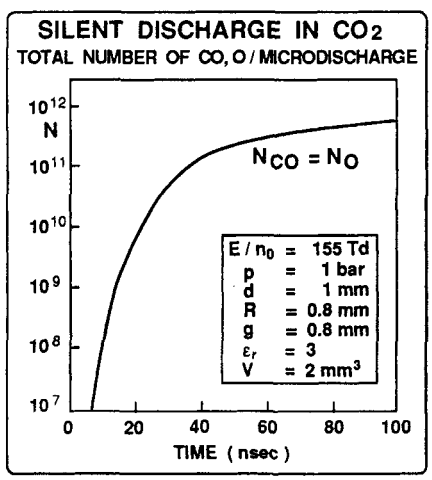


Fig. 12: Total number of CO molecules formed during a microdischarge.

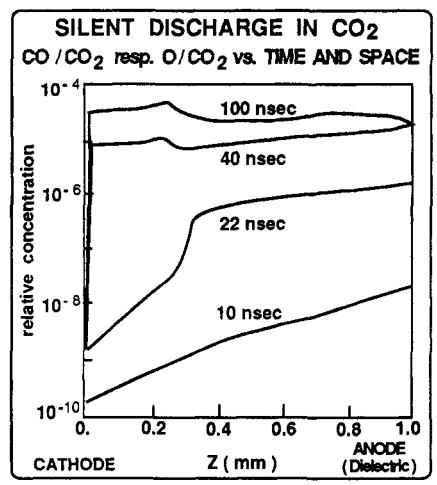


Fig. 13: Axial variation of average CO concentration at different times during microdischarge evolution.

## APPLICATIONS OF DIELECTRIC BARRIER DISCHARGES

All applications of DBDs follow a general scheme. The applied electric field initiates a discharge in which charged particles, excited species and free radicals are formed. Further reactions of these unstable species lead to chemical changes in the process gas. Depending on the desired application different reaction mechanisms may be of importance.

### Ozone Generation

The first and still the most important application of DBDs is the generation of ozone from air or from oxygen. The first larger ozone generating facilities for the disinfection of drinking water were built in Nice (France) and in St.Petersburg (Russia) at the turn of this century. Today, a few thousand installations are in operation. The largest ones reach power levels of several MW and produce some tons of ozone per day. Although the purification of potable water is still the most important ozone market other applications have emerged. Examples are the conditioning of cooling water circuits, the treatment of waste waters as well as large-scale chemical oxidation and bleaching processes. A major ozone application for the future is expected as a substitute for chlorine in pulp bleaching.

Ozone synthesis in DBDs starts with the very efficient dissociation of oxygen molecules by electron impact (Fig. 7). The generated oxygen atoms can follow different reaction paths.

$$O + O_2 + M \rightarrow O_3^* + M \rightarrow O_3 + M \qquad (2)$$

$$O + O + M \rightarrow O_2 + M \qquad (3)$$

$$O + O_3^* \rightarrow 2\,O_2 \qquad (4)$$

$$O + O_3 \rightarrow 2\,O_2 \qquad (5)$$

In these reactions M is a third collision partner which can be an oxygen molecule, in air also a nitrogen molecule. $O_3^*$ is an intermediately formed excited ozone molecule which is much more reactive than the ground state of ozone ($O_3$). The relative importance of the different reactions depends on the relative particle concentrations, the pressure and the gas temperature. Reaction (2) is favoured at reasonably high pressure (1 - 3 bar), low gas temperatures and relatively low atom concentrations ($[O]/n \sim 10^{-3}$). The first two requirements necessitate a nonequilibrium discharge because the electrons need a sufficiently high energy to dissociate oxygen molecules efficiently (Fig. 7). The DBD with narrow discharge gaps can fulfil all these requirements in an almost ideal way (16-19, 45, 66, 67).

Because of the high cost of pure oxygen many smaller ozone generators use air as a feed gas. However, this solution has several drawbacks. Since humidity interferes adversely with the DBD operation and the ozone formation process the air has to be dried to a dew point of -60 °C, which corresponds to a residual $H_2O$ content of a few ppm. A second disadvantage is that the dissociation of oxygen molecules in air is much less efficient because vibrational excitation and dissociation of nitrogen molecules takes up a major fraction of the electron energy (56, 68). However, not all of this energy is lost because some reactions involving nitrogen atoms N and excited nitrogen molecules $N_2^*$ can lead to the formation of additional oxygen atoms which, in turn, can react to form ozone (67, 69).

$$N + O_2 \rightarrow NO + O \qquad (6)$$

$$N + NO \rightarrow N_2 + O \qquad (7)$$

$$N_2^* + O_2 \rightarrow N_2 + 2\,O \qquad (8a)$$

$$\rightarrow N_2O + O \qquad (8b)$$

The general experience is that ozone generators operating on air need twice the specific energy for a certain amount of ozone and reach about half the concentration of ozone generators operating with oxygen. As a third disadvantage the appearance of nitrogen oxides ($N_2O$, NO, $NO_2$, $NO_3$, $N_2O_5$) has to be mentioned which renders the optimization of the discharge process much more complicated than that in pure oxygen. As a matter of fact, technical ozone generators operating on air require different operating conditions for optimum performance.

### Excimer Lamps

The electron densities and electron energies reached within the microdischarges are comparable to those of discharge-pumped excimer lasers. Consequently, it is possible to use DBDs in rare gases or mixtures of

rare gases and halogens, for example, to form excimers. Since many excimers are efficient fluorescers powerful ultraviolet and vacuum ultraviolet sources can be based on this principle (24-28, 43, 70,71).
Two examples of excimer formation in DBDs will be given: The formation of $Xe_2^*$ excimers radiating at 172 nm in the vacuum UV range and the formation of $XeCl^*$ excimers radiating at 308 nm in the UV-B range. $Xe_2^*$ is formed from excited xenon atoms $Xe^*$, $XeCl^*$ mainly by ion recombination. Both processes are three-body reactions requiring a fairly high pressure:

$$Xe^* + Xe + M \rightarrow Xe_2^* + M \quad (9) \qquad Cl^- + Xe^+ + M \rightarrow XeCl^* + M \quad (10)$$

In these reactions M stands for a third collision partner, in many cases, an atom of an additional rare gas used as a buffer gas to influence the electron energy distribution.
Contrary to the common practice in excimer lasers the gas mixture can be sealed in quartz vessels and operated for an extended period of time. An important advantage of these lamps is that the electrodes are not in contact with the discharge plasma and, consequently, the build up of contaminants due to electrode attack is avoided.
Using different gas mixtures narrow-band excimer fluorescence was obtained for more than 20 different wavelengths between 100 nm and 550 nm (72). In many cases it is possible to obtain a single dominant emission band by carefully adjusting gas composition and pressure. Typical spectral widths at half intensity range from 1 nm to 15 nm. Since excimer mixtures can be pumped at high power densities it is possible to build very powerful, spectrally selective sources of UV photons to initiate photochemical and photophysical processes. A number of novel procedures including high-speed UV curing, the photodeposition of metallic, insulating and semiconducting layers as well as photoetching of polymer surfaces have already been demonstrated with these DBD excimer lamps (26-28, 73-77). Future applications are foreseen utilizing UV induced photodegradation and photooxidation processes for pollution control (78, 79).

### Miscellaneous Applications

In recent years considerable attention has been given to the use of dielectric barrier discharges for the reduction of NOx and SOx in flue gases, for the treatment of volatile organic compounds (VOCs) in off-gases, or stripped from contaminated liquids or soils (29-31, 38). In addition, the treatment of formaldehyde (37) and even of pesticides and nerve gases has been suggested (17, 35, 36). In these applications the DBD plasma generates ions and radicals which can result in an efficient reduction of pollutant concentration. In many cases the species $O(^3P)$, $O(^1D)$, H, N, in wet air also $HO_2$ and OH radicals, initiate fast, in some cases highly selective, chemical reactions.
The decomposition of $H_2S$ has also been investigated (39). The DBD was operated at unusually high temperatures of up to 560 °C in order to remove the sulfur in liquid or vapour form. $H_2S$ is found in many natural gas sources and has to be taken out. As the amounts that have to be treated can be quite large this process could be of considerable technical importance. If $H_2S$ could be decomposed into S and $H_2$ at a reasonable energy expenditure valuable products could be obtained.
Other recent investigations focus on the potential of DBDs for surface processes. The work of Okazaki et al. (32, 42) and of Massines et al. (34) has been oriented towards obtaining homogeneous discharges, referred to as **a**tmospheric **p**ressure **g**low discharges or APGs, for thin film deposition, surface modification and dry etching processes. On the other hand, also inhomogeneous DBDs with pronounced microdischarge activity can be utilized for surface treatment (33). As a matter of fact, the well established "corona treatment" of plastic parts and polymer foils, in most cases, uses a DBD configuration.
Another industrial application of DBDs is Mitsubishi's silent discharge or SD $CO_2$ laser (20-22). In this case large gap spacings and plane dielectrics covering cooled planar electrodes are used. The gas mix ($CO_2$, CO, $N_2$, He), the low pressure of 6 kPa together with a strong transverse gas flow result in a diffuse, almost homogeneous discharge. Using special optical resonators practically diffraction limited output beams of 5 - 10 kW average power can be obtained. This SD $CO_2$ laser is a powerful tool for high speed welding and cutting.

### Future Applications: $CO_2$ Hydrogenation

The issue of global climate change, especially the possibility of a warming of the surface of the earth due to emissions of so-called man-made greenhouse gases, is of great importance for the future development of

energy and power technologies. The forecasts for the development of energy use and emissions predict a 50% increase of the use of energy and $CO_2$ emissions before the year 2010. This increase will mostly come from the developing countries. If a direct cause and effect relationship can be proven between emissions of man-made gases and warming of the atmosphere, - and this might happen within the next decade -, then it is quite likely that technological options for mitigating the emissions will be called for.
About a third of the global man-made emissions of $CO_2$ come from power plants. One possible way of reducing $CO_2$ output would be recycling $CO_2$ taken from flue gases of power plants. The removal of $CO_2$ from flue gases is already being done in a 300 MW coal-fired power plant, which was built by ABB Lummus Crest at Shady Point in Oklahoma. Every day 200 tons of $CO_2$ are removed from the flue gases. This is only a small portion of the total amount of $CO_2$ generated. The $CO_2$ is very pure and it is used in the food industry. The total market for such use of $CO_2$ however, is very limited.
One possible utilization of $CO_2$ on a large scale is the conversion of $CO_2$ with the aid of hydrogen to form hydrocarbons like e.g. methane or methanol (80). The key to hydrogenation of $CO_2$ is, of course, the availability of hydrogen. The hydrogen would have to be produced in a $CO_2$-free way, e.g. by using solar energy, hydro energy, nuclear energy or biomass and reforestation. $CO_2$ has a very low energy content. Because of the energy needed to convert it to e.g. methanol, such conversion would presumably only be considered if other motivating forces were active, like e.g. the introduction of a carbon tax.
There is also another use for $CO_2$ which might turn out to be of no less importance. An important role has been predicted for the future for hydrogen as a clean source of energy. Hydrogen is a gas at normal temperature and pressure and cannot efficiently be stored. Methanol, on the other hand, is a liquid under normal conditions. Methanol, produced by combining carbon dioxide and hydrogen, could thus be used as storage medium for hydrogen in general and for hydrogen produced during the day by solar energy, in particular. There is also an added advantage. Methanol has almost twice the energy content per volume in comparison to that of liquid hydrogen.
The reaction of carbon dioxide with hydrogen to form methanol is an exothermic reaction (81):

$$CO_2 + 3H_2 \rightarrow CH_3OH + H_2O \qquad (11)$$

Reaction (11) needs to be activated by a catalyst, though (83). The catalyst operates at temperatures around 500 K.
The formation of hydrogen itself is an endothermic process. In case of water electrolysis it requires an input of somewhat less than 5 $kWh/m^3H_2$. (84)

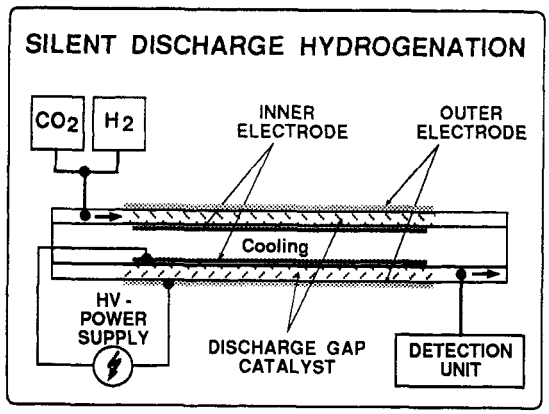


Fig. 14: Annular dielectric barrier discharge configuration for $CO_2$ hydrogenation.

Reaction (11) can also be activated in a discharge (40, 41, 81, 82) as shown in Fig. 14. Instead of using a catalyst one can activate $CO_2$ and $H_2$ according to:

$$e + CO_2 \rightarrow CO_2^* + e \qquad (12) \qquad e + H_2 \rightarrow H_2^* + e \qquad (13)$$

The molecules thus excited can then initiate reactions like reaction (11). The excited molecules can also form other products like methane according to:

$$CO_2 + 4\,H_2 \rightarrow CH_4 + 2\,H_2O \qquad (14)$$

Fig. 15 shows the temporal development of different species during a series of microdischarges in 20% $CO_2$ and 80% $H_2$ at 1 bar and 400 K. The time interval between pulses was 12.5 ms. In Fig. 16 we show a comparison of measured and calculated concentrations of $CH_4$, CO and $CH_3OH$. The experiment was performed at 1 bar and 400 K. The feed consisted of a mixture of $CO_2$ and $H_2$ and the reaction time was 6 minutes. The calculation considered 576 discrete pulses during this time.

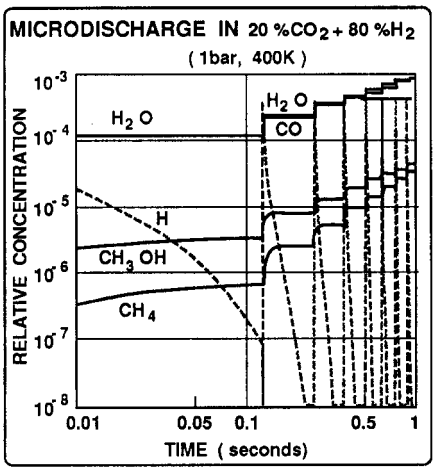


Fig. 15: Chemical changes due to a series of microdischarges.

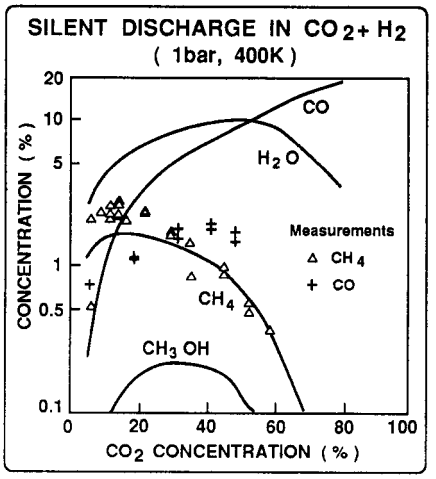


Fig. 16: Comparison of calculated and measured species concentrations during $CO_2$ hydrogenation.

The silent discharge provides electrons at energies which are ideal for dissociating molecules. There are many abundant sources of hydrogen e.g. water ($H_2O$), hydrogen sulfide ($H_2S$), methane ($CH_4$). Due to the dissociation capability of the silent discharge one can consider making the hydrogen necessary for the hydrogenation of the $CO_2$ directly in the discharge itself. One would e.g. combine water vapour and carbon dioxide and obtain the hydrogen required from:

$$e + H_2O \rightarrow 2\,H + O + e \rightarrow H_2 + 1/2\,O_2 + e \qquad (15)$$

At the same time the molecular species present in the discharge would be in an excited state such that perhaps no catalyst would be necessary for reaction (11). Needless to say, there would be no problem in introducing a catalyst into the discharge gap (Fig. 14). It is quite likely that the combination of a DBD and an appropriate catalyst will improve the performance of the DBD reactor quite considerably (plasma assisted catalysis PAC).

These experiments are very preliminary and the results are far from indicating an economic solution. But they demonstrate the possibility of converting $CO_2$ in DBDs and may be regarded as a step towards tackling the $CO_2$ problem.

## SUMMARY AND OUTLOOK

It has been shown how electrical breakdown - which leads to the formation of microdischarges in high pressure gases - and the atomic and molecular excitation - which initiates the ensuing chemistry - can be combined in one numerical model of dielectric barrier discharge chemistry. In these discharges large gas flows at atmospheric pressure can be subjected to nonequilibrium plasma conditions. The reliability and efficiency of this discharge technology has been demonstrated in industrial ozone generation. Further large-scale applications are foreseen in the fields of plasmachemical synthesis, pollution control and surface modification. The more recent applications of DBDs to generate powerful coherent radiation in $CO_2$ lasers

as well as incoherent excimer radiation in UV lamps is also expected to find widespread industrial applications. Further research might even lead to $CO_2$ hydrogenation in DBDs. It thus appears that dielectric barrier discharges, more than a century after their first introduction, are gaining an ever increasing importance in a variety of applications.

Acknowledgement: Special thanks are due to M. Yousfi for making available his data collection on $CO_2$ cross sections.

REFERENCES

1. W. Siemens. *Poggendorffs Ann. Phys. Chem.* **102**, 66 (1857).
2. T. Andrews and P.G. Tait. *Phil. Trans. Roy. Soc. London* **150**, 113 (1860).
3. P. Hautefeuille and J. Chappius. *Compt. Rend.* **92**, 80 (1881).
4. E. Warburg and G. Leithäuser. *Ann Physik.* (4) **28**, 313 (1909).
5. E. Warburg. *Ann. Physik.* (4) **13**, 464 (1904).
6. E. Warburg. *Z. tech. Phys.* **6**, 625 (1925).
7. H. Becker. *Wiss. Veröff. Siemens-Konz.* **1**, 76 (1920).
8. H. Becker. *Wiss. Veröff. Siemens-Konz.* **3**, 243 (1923).
9. M.-P. Otto. *Bull. Soc. Franç. Electr.* **9**, 129 (1929).
10. E. Briner and b. Susz. *Helv. Chim. Acta.* **13**, 678 (1930).
11. Yu. V. Filippov, V.A. Boblikova and V.I. Panteleev. *Electrosynthesis of Ozone (Russ.). Moscow State University* (1987).
12. J.C. Devins. *J. Electrochem. Soc.* **103**, 460 (1956).
13. R.W. Lunt. *Advances in Chemistry Series.* ***21***, 286 (1959).
14. S. Fuji and N. Takemura. *Advances in Chemistry Series.* ***21***, 334 (1959).
15. V.G. Samoilovich, V.I. Gibalov and K.V. Kozlov. *Physical Chemistry of the Barrier Discharge (Russ.). Moscow State University* (1989).
16. B. Eliasson and U. Kogelschatz. *IEEE Trans. Plasma Sci.* **19**, 309 (1991).
17. B. Eliasson and U. Kogelschatz. *IEEE Trans. Plasma Sci.* **19**, 1063 (1991).
18. U. Kogelschatz. *Proc. XVI. Int. Conf. on Phenomena in Ionized Gases.* Invited Papers, p. 240, Düsseldorf (1983).
19. U. Kogelschatz. *Proc. Tenth Int. Conf. on Gas Discharges and their Applications*, p. 972, Swansea (1992).
20. S. Yagi and N. Tabata. *Proc. IEEE/OSA Conf. on Lasers and Electro-Opt.* Paper WE **5**, p. 22, Washington DC (1981).
21. K. Yasui, M. Kuzumoto, S. Ogawa, M. Tanaka and S. Yagi. *IEEE J. Quantum Electron.* **25**, 836 (1989).
22. Y. Takenaka, M. Kuzumoto, K. Yasui, S. Yagi and M. Tagashira. *IEEE J. Quantum Electron.* **27**, 2482 (1991)
23. A.K. Shuaibov and V.S. Shevera. *Sov. Phys.-Tech. Phys.* **24**, 976 (1979).
24. G.A. Volkova, N.N. Kirillova, E.N. Pavlovskaya and A.V. Yakovleva. *J. Appl. Spectrosc.* **41**, 1194 (1984).
25. B. Eliasson and U. Kogelschatz. *Appl. Phys.* **B 46**, 299 (1988).
26. U. Kogelschatz. *Pure & Appl. Chem.* **62**, 1667 (1990).
27. U. Kogelschatz. *Proc. XX. Int. Conf. on Phenomena in Ionized Gases.* Invited Papers, p. 953, Pisa (1991).
28. U. Kogelschatz. *Appl. Surf. Sci.* **54**, 410 (1992).
29. I. Sardja and S.K. Dhali. *Appl. Phys. Lett.* **56**, 21 (1990).
30. M.B. Chang, J.H. Balbach, M.J. Rood and M.J. Kushner. *J. Appl. Phys.* **69**, 4409 (1991).
31. M. B. Chang, M.J. Kushner and M.J. Rood. *Plasma Chem. Plasma Proc.* **12**, 565 (1992).
32. S. Kanazawa, M. Kogoma, T. Moriwaki and S. Okazaki. *J. Phys. D: Appl. Phys.* **21**, 838 (1988).
33. U. Reitz. *Barrierententladungen zur plasmagestützten Oberflächenbehandlung.* Dissertation. TU Braunschweig (1992).
34. F. Massines, C. Mayoux, R. Messaoudi, A. Rabehi and P. Ségur. *Proc. Tenth Int. Conf. on Gas Discharges and their Applications.* p.730 (Swansea 1992).
35. E.J. Clothiaux, J.A. Koropchak and R.R. Moore. *Plasma Chem. Plasma Proc.* **4**, 15 (1984).
36. R.S. Sheinson and N.S. Smyth. *Proc. 8th Int. Symp. on Plasma Chem.* p. 648 Tokyo (1987).
37. D.G. Storch and M.J. Kushner. *J. Appl. Phys.* **73**, 51 (1993).
38. W.H. McCulla, L.A. Rosocha, W.C. Neely, E.J. Clothiaux, M.J. Kushner and M.J. Rood. *Treatment of hazardous organic wastes using wet air plasma oxydation. Proc. 1st INEL Plasma Applications to Waste Treatment Workshop,* Idaho Falls (1991).

39. I. Traus and H. Suhr. *Plasma Chem. Plasma Proc.* **12**, 275 (1992).
40. B. Eliasson, F.-G. Simon, W. Egli and P. Brunner. *Helv. Phys. Acta.* **65**, 129 (1992).
41. W. Egli and B. Eliasson. *Helv. Phys. Acta.* **65**, 127 (1992).
42. T. Yokoyama, M. Kogoma, S. Kanazawa, T. Moriwaki and S. Okazaki. *J. Phys. D: Appl. Phys.* **23**, 374 (1990).
43. V. Schorpp. *Die dielektrisch behinderte Edelgas-Halogen-Excimer-Entladung: Eine neuartige UV-Strahlenquelle.* Dissertation. Karlsruhe University (1991).
44. M. Kogoma, S. Okazaki, N. Kanda, H. Uchiyama and H. Jinno. *Proc. Jpn. Symp. Plasma Chem.* **4**, 345 Tokyo (1991).
45. D. Braun, U. Küchler and G. Pietsch. J. Phys. D: Appl. Phys. *24, 564 (1991).*
46. D. Braun, V. Gibalov and G. Pietsch. *Plasma Sources Sci. Technol.* **1**, 166 (1992).
47. B. Eliasson and S. Straessler. *Bull. Amer. Phys. Soc.* **28**, 183 (1983).
48 V.I. Gibalov, J. Drímal, M. Wronski and V.G. Samoilovich. *Contrib. Plasma Phys.* **31**, 89 (1991).
49. A.V. Phelps and S.A. Lawton. *J. Chem. Phys.* **69**, 1055 (1978).
50. N.P. Penkin, V.V. Smirnov and O.D. Tsygir. *Sov. Phys.-Tech. Phys.* **27**, 945 (1982).
51. A.V. Phelps. *JILA Information Center Report* No. 28. Boulder (1985).
52. B. Eliasson and U. Kogelschatz. *J. Phys. B.: At. Mol. Phys.* **19**, 1241 (1986).
53. P.C. Cosby. *J. Chem. Phys.* **98**, 9560 (1993).
54. W.L. Nighan. *Phys. Rev.* **A2**, 1989 (1970).
55. A.N. Lobanov and A.F. Suchkov. *Sov. J. Quant. Electron.* **4**, 843 (1975).
56. H.N. Kücükarpaci and J. Lucas. *J. Phys. D: Appl. Phys.* **12**, 2123 (1979).
57. M. Braglia, R. Winkler and J. Wilhelm. *Contrib. Plasma Phys.* **31**, 463 (1991).
58. M. Yousfi. Private Communication
59. I. Gallimberti. *J. Phys. D: Appl. Phys.* **5**, 2179 (1972).
60. E.D. Lozanskii. *Sov. Phys.-Usp.* **18**, 893 (1976).
61. E.E. Kunhardt and W.W. Byszewski. *Phys. Rev.* **21**, 2069 (1980).
62. V.I. Gibalov, V.G. Samoilovich and Yu.V. Filippov. *Sov. J. Phys. Chem.* **55**, 471 (1981).
63. R. Morrow. *Phys. Rev.* **A 35**, 1778 (1987).
64. S.K. Dahli and D.F. Williams. *J. Appl. Phys.* **62**, 4696 (1987).
65. B. Eliasson and W. Egli. *Helv. Phys. Acta.* **60**, 241 (1987).
66. B. Eliasson, M. Hirth and U. Kogelschatz. *J. Phys. D: Appl. Phys.* **20**, 1421 (1987).
67. U. Kogelschatz. *Advanced Ozone Generation,* in: *Process Technologies for Water Treatment* (S. Stucki, ed.) p.87, Plenum Press, New York (1988).
68. G. Fournier, J. Bonnet and D. Pigache. *C.R. Acad. Sc. Paris.* **290**, B 179 (1980).
69. B. Eliasson, U. Kogelschatz and P. Baessler. *J. Phys. B: Atom. Mol. Phys.* **17**, L797 (1984).
70. B. Gellert. *Contrib. Plasma Phys.* **31**, 247 (1991).
71. K. Stockwald. *Neuartige Xenon- und Xenon/Quecksilber-Lampen im VUV/UV-Spektralbereich.* Dissertation. Karlsruhe University (1991).
72. B. Gellert und U. Kogelschatz. *Appl. Phys.* **B52**, 14 (1991).
73. H. Esrom, J. Demny and U. Kogelschatz. *Chemtronics.* **4**, 202 (1989).
74. U. Kogelschatz, B. Eliasson and H. Esrom. *ABB Review.* **3/91**, 21 (1991).
75. F. Kessler and G.H. Bauer. *Appl. Surf. Sci.* **54**, 430 (1992).
76. P. Bergonzo, U. Kogelschatz and I.W. Boyd. *Appl. Surf. Sci.* **69**, 393 (1993).
77. H. Esrom and U. Kogelschatz. *Thin Solid Films.* **218**, 231 (1992).
78. U. Kogelschatz. *UV production in dielectric barrier discharges for pollution control. Proc. NATO Adv. Res. Workshop on Non-Thermal Plasma Techniques for Pollution Control.* Cambridge (1992).
79. H. Scheytt, H. Esrom, L. Prager, R. Mehnert and C. von Sonntag. *Ultraviolet light and electron beam induced degradation of trichloroethylene. Proc. NATO Adv. Res. Workshop on Non-Thermal Plasma Techniques for Pollution Control. Cambridge (1992).*
80 T. Inui and T. Takeguchi. *Catalysis Today.* **10**, 95 (1991).
81. B. Eliasson, F.-G. Simon and W. Egli. *Hydrogenation of $CO_2$ in a Silent Discharge.* ABB Corporate Research Report **CRB-92-002 C.** Baden-Dättwil (1992).
82. B. Eliasson, F.-G. Simon and W. Egli. *Hydrogenation of $CO_2$ in a silent discharge. Proc. NATO Adv. Res. Workshop on Non-Thermal Plasma Techniques for Pollution Control.* Cambridge (1992).
83. C. Schild, A. Wokaun and A. Baiker. *J. Molec. Catalysis.* **63**, 223 and 243 (1990).
84. C.J. Winter and J. Nitsch (eds.). *Wasserstoff als Energieträger.* p. 178, Springer, Berlin (1986).